Available online at www.sciencedirect.com

ScienceDirect

Advances in Space Research 69 (2022) 3236–3244

ADVANCES IN SPACE RESEARCH (a COSPAR publication)

www.elsevier.com/locate/asr

Wave variability along the world's continental shelves and coasts: Monitoring opportunities from satellite Earth observation

Erwin W.J. Bergsma [a,*], Rafael Almar [b], Edward J. Anthony [c], Thierry Garlan [d], Elodie Kestenare [b]

[a] Earth Observation Lab, CNES, 18 Av. Edouard Belin, 31400 Toulouse, France
[b] IRD-LEGOS, UMR5566, 14 Av. Edouard Belin, 31400 Toulouse, France
[c] Aix Marseille Univ, CNRS, IRD, INRA, Coll France, CEREGE, Aix-en-Provence, France
[d] SHOM, Dpt. of Marine Geology SHOM, Brest, France

Received 16 February 2021; received in revised form 13 January 2022; accepted 24 February 2022
Available online 1 March 2022

Abstract

Insight on wave regimes along the world's coastlines is important for virtually all coastal and nearshore marine activities, installations, planning and protection. Waves are pervasive and the dominant source of energy driving extreme sea levels, the transport of pollutants and sediments, erosion, and a major contributor to risks of flooding. We quantify the global spatio-temporal wave conditions along the world's coasts and evaluate the needs for coastal Earth Observation strategies, with the aim, notably, that the derived scales of change can contribute to optimisation of these strategies. A global dominant timescale of 30 days is found in coastal wave variability that is, on average, spatially correlated just over the synoptic 5 degrees' regional scale (≈ 550 km at the equator). This regional-scale dimension suggests that the timing and design of traditional field surveys and observations relevant to a vast array of coastal activities, and which may be expensive in terms of human resources, may be complemented by information gained from satellite Earth Observation that throws light on spatio-temporal scales of wave-energy change along the world's coastlines.

Keywords: Wave variability; Coastal observations; Seasonality; Satellite monitoring

1. Introduction

As vectors of global energy transmission from the oceans to the coast (Reguero et al., 2015), ocean waves are a fundamental component of coastal and nearshore systems. Being products of ocean–atmosphere interaction, ocean waves are variable and exhibit spatial and temporal scales that are driven by well-known regional climate patterns (Young et al., 2011; Stopa and Cheung, 2014). One early attempt at the spatial and temporal characterisation of wave patterns along the world's coasts was that of Davies (1980), who identified various global wave environments from the tropics to the poles, notably swell and trade-wind affected coasts.

Insight on spatial and temporal patterns of wave regimes along the world's coastlines is important for virtually all shore- and nearshore-based activities such as tourism, fishing, infrastructure and engineering such as placement of coastal sand nourishment, ports, communication cables and pipelines, resource-tapping such as mining, wind and marine power extraction, oil extraction, archaeology, habitats and their protection, and plastic and contaminant transport and deposition. Knowledge of coastal wave regimes is, thus, important in aiding decision-making regarding spatial planning and protection and

* Corresponding author.
E-mail address: erwin.bergsma@cnes.fr (E.W.J. Bergsma).

https://doi.org/10.1016/j.asr.2022.02.047
0273-1177/

dealing with marine hazards. Similarly, information on the spatio-temporal variability of wave regimes allows for a usability judgement of current available Earth Observation data as well as forming a base argumentation for future satellite missions and their required revisit times for effective monitoring of the coastal zone (Ardhuin et al., 2019).

Coastal waves cover a wide range of coastal environments worldwide, as summarised in Fig. 1 following Davies (1980). In the mid-latitudes, storm-driven winter ocean waves imply a strong seasonality (Davidson et al., 2013; Masselink et al., 2016; Bergsma et al., 2019b). Similarly, in tropical regions, seasonal effects are induced by monsoons and by typhoon passages that can determine coastal environmental variability (Jeanson et al., 2013; Almar et al., 2017; Anthony et al., 2017; Ariffin et al., 2018). Large stretches of tropical storm-free eastern coasts, distant from wave generation, are under the influence of mid-to-high latitude western incidence swells (Boucharel et al., 2021). Tropical western coasts are conversely largely exposed to trade wind-generated waves with their own variability. Extreme tropical cyclones are also a dominant forcing for waves in various closed environments. Lastly, protected areas (such as small basins, sheltered areas and ice-capped coasts in high latitudes) have a singular behaviour with a predominant exposure to short-crested fetch limited waves and extreme winds in the absence of long distant swell waves.

Coastal environments are thus potentially exposed to wave-energy variability over a wide range of timescales, from storm events, seasonal and interannual to decadal and longer. The timing of any observation strategy generally gives an instantaneous picture of the state of the coastal system one observes (Benveniste et al., 2019; Melet et al., 2020). At the same time, there is no doubt that frequent coastal monitoring at scales of days to weeks, and even sometimes months, whatever the objective and the domain of application, is not only costly but often unrealistic. For example, storm-induced extreme surges and subsequent coastal flooding occur at a timescale of hours (Almar et al., 2021c), and it is, therefore, easier and more reasonable to set up strategies that capture changes over a series of storms, typically over a winter, for instance (Masselink et al., 2016; Castelle et al., 2021). A better understanding of wave variability as a prime element of coastal seasonality and a primary driver of coastal hazards and morphological and ecosystem changes can usefully contribute to choices in survey timing aimed at improving the ratio gain/effort on data. Space-borne, Earth Observation techniques, covering large areas on a global scale, can be a useful tool in assessing the relationship between wave patterns and morphological changes (Benveniste et al., 2019; Turner et al., 2021), for instance. Nonetheless, the application of these emerging techniques at the global scale is also costly in terms of processing time, computational effort and storage, though they are becoming more and more accessible to the scientific community and other parties interested in coasts and the nearshore zone. In this paper, we quantify wave regime spatio-temporal scales along the world's coasts, put current survey strategies in perspective, and frame new opportunities offered by satellite earth observation to address these challenges.

2. Methods

We use the ERAInterm global re-analysis (Dee et al., 2011) to determine wave variability. From the ERAInterm 0.5x0.5° resolution database, 6-hourly wave heights and energy periods are extracted along the world's coasts (equally spaced over 14,140 points) covering a 24 years from January 1993 to January 2017. From these parameters the offshore wave energy flux (in other words, wave power) is computed as shown in Eq. 1 so that for each of the 14140 points we have a 24-year time-series of incident wave energy flux (*Ef*).

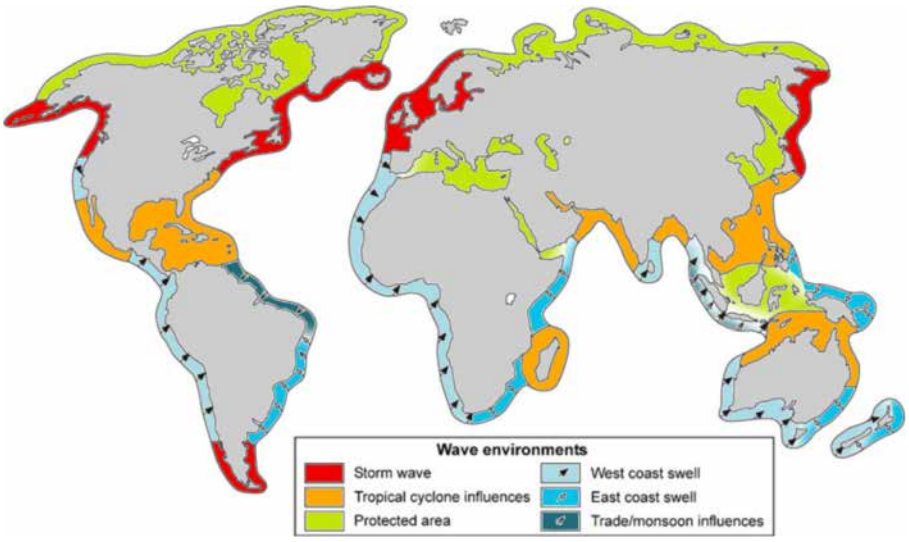

Fig. 1. Coastal wave environments worldwide, from Davies (1980)).

$$Ef = \frac{\rho g^2}{64\pi} H_s^2 T_e \quad (1)$$

In which ρ refers to water density (a global value of 1025 kg/m^3 is used), g represents gravitational acceleration (for which a global value of 9.8 is used), H_s the significant wave height and T_e the corresponding wave energy period. Noteworthy, local detailed inshore waves conditions are complex (Passaro et al., 2021a) and out of the reach (and scope) of this study that is global and necessarily coarse. We aim here at resolving the regional to global scales of coastal scale wave-forcing variability solely not the amplitude of the subsequent numerous and various processes that might include non-linearities and interplays within the coastal system (Anthony and Aagaard, 2020). The observational time-interval (Δt_{obs}) determines to a great extent which timescales one can resolve for. Here we analyse the effect of increasingly sparser sampling in terms of uncertainty (level of high-frequency signal not captured). If we capture the signal at our maximum temporal resolution (6 h), the full wave variability potential is observed (limited by our dataset), resulting in 0% uncertainty in observing the signal. Subsequently, the sampling frequency is decreased and the captured uncertainty increases. Instead of taking an absolute Δt diminishing the number of data points, we decrease the sampling frequency by enlarging the running average window, Δt_{obs} in Eq. 2.

$$\text{Uncertainty} = \frac{\sigma\left(Ef - \frac{1}{\Delta t_{obs}} \sum_{i=-\Delta t_{obs}/2}^{\Delta t_{obs}/2} Ef_i\right)}{\sigma(Ef)} \quad (2)$$

in which σ is the standard deviation, Δt_{obs} time interval between observations and Ef incident wave energy flux. Depending on the wave climate and its temporal variations, the uncertainty increases either rapidly or remains low for longer time intervals and finally, a plateau emerges before 100% uncertainty is reached. An optimal time interval is defined as the moment that the time interval becomes as large as possible without a further loss of certainty. This point is indicated by the vertical green line in Fig. 2. For example, wave environments with relatively little seasonality gain uncertainty rapidly while for wave climates with a clear seasonality the uncertainty remains low for longer timescales. What we will see below is that the uncertainty often increases significantly between a high-frequency data sampling rate (every 6 h) and the week time-interval: on average 60–80% (so we observe 20–40% of the variability), as illustrated in Fig. 2.

The spatial correlation was then computed at different timescales, using a pass-band filter over wave time-series to correlate daily wave regimes spatially. A distance threshold was applied to the spatial correlation results to determine the representative distance of correlation.

3. Results

3.1. Dominant spatio-temporal scales of coastal waves

We can start by looking at the dominant temporal scales of coastal wave energy data from hindcasts. A global wave energy timescale map is shown in Fig. 3 with global mean and median timescales of respectively 48 days and 2 weeks. Local details can be found in the supplementary material (Fig. S1). The global representation in Fig. 3a shows clustering patterns. At mid to high latitudes, 45° to 60°, monthly to bi-monthly timescales linked to Westerly storm tracks are found. In the Southern Ocean, continuous Westerly storm tracks result in short – weekly – timescales only, e.g. at the coasts of Patagonia, South Africa, Southern Australia and New Zealand. In contrast, in the North Atlantic and North Pacific Oceans, Westerly storm-tracks (Hoskins and Hodges, 2019a; Hoskins and Hodges, 2019b) result in storm-season dominated west coasts (Western Europe and West coast of Northern America) and short (about bi-weekly) wave-energy timescales along the east coasts of North America, Russia and Japan. The inter-tropical band has strong seasonality and exhibits dominant longer timescales in the order of bi-monthly to seasonal. These can be linked to the dominance of monsoon/trade-wind seasons and related ocean waves as well as longer swell arriving from higher latitudes (Davies, 1980; Hoskins and Hodges, 2005; O'Kane et al.,

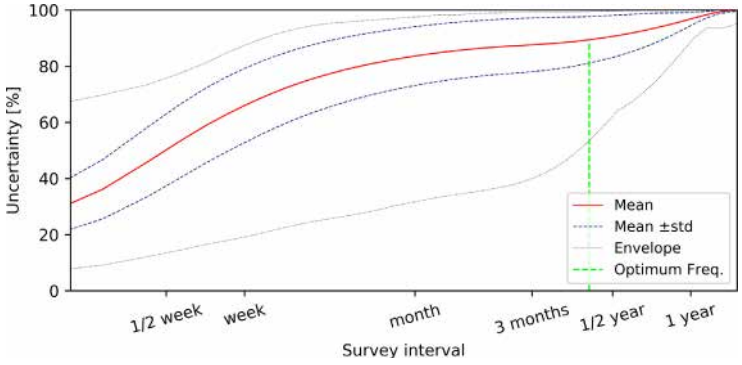

Fig. 2. Worldwide average uncertainty distribution per survey interval including the standard deviation (dashed blue lines) and envelope (dotted light grey lines). The green dashed line represents the optimal surveying frequency.

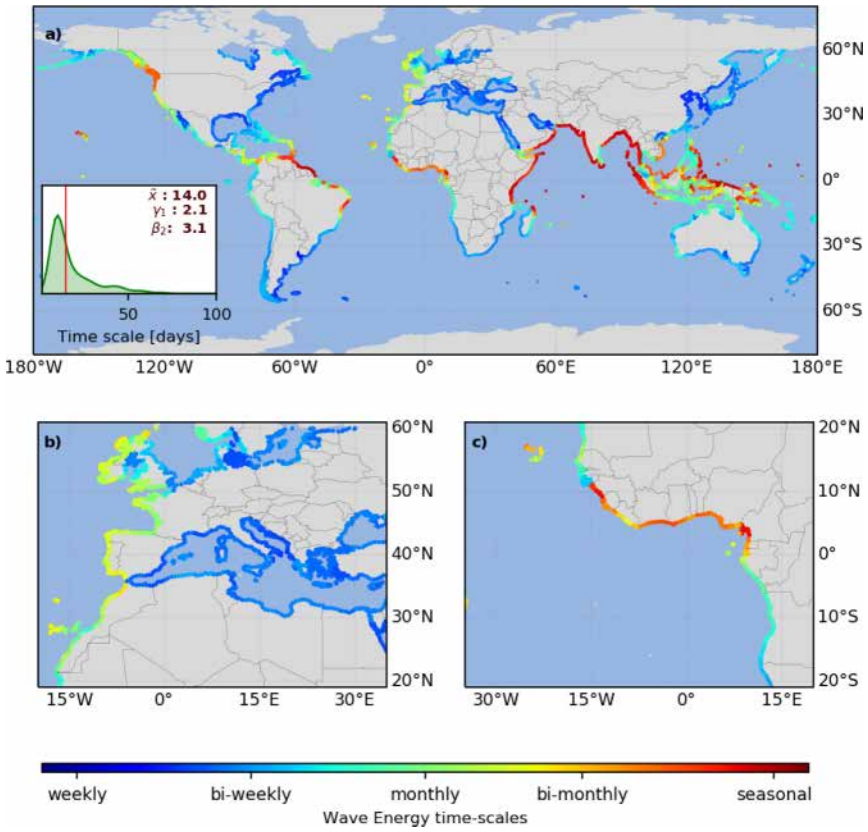

Fig. 3. Global coastal wave variability time-scales (a) and two zooms; (b) part of Europe and Northern Africa, and (c) a part of Western Africa. The logarithmic colour map covers time-scales from a few days to seasonal. Longer timescales seem never to dominate. The insert in (a) represents a distribution of the global timescales. The red vertical line in the insert indicates the median global value for time-scales.

2014). Closed or protected seas/gulfs such as the Mediterranean Sea, the Black Sea, the Persian Gulf, the Sea of Japan or the Gulf of Mexico experience, predominantly, exposure to locally generated wind waves, hence the dominant short wave-energy timescales.

In Fig. 3b,c we illustrate the clustering by zooming in on mid-latitude storm-dominated European coasts (b) and equatorial to tropical Western Africa (c). Fig. 3b shows a coherent change timescale behaviour around Europe's coasts. At the Atlantic coast, exposed to ocean swells, a seasonal signal is found in the incident wave energy flux. This seasonal fluctuation in the wave energy flux implies that uncertainty remains low over significantly longer timescales, hence the monthly to bi-monthly timescales. In the Mediterranean Sea, sheltered from ocean swells, locally generated wind waves dominate, as stated above. Short-crested low period waves (which are punctual and show little long-term fluctuations) are typically found in this sea, resulting in dominant short wave-energy timescales.

For Western Africa (Fig. 3c), an apparent North-to-South shorter-longer shift in timescales can be found at 20 to 10° N, 10° N to 0°, and 0° to 20° S. Between 20° and 10° N, short timescales can be assigned to the combination of Northerly and Southerly swell (Abessolo Ondoa et al., 2017; Sadio et al., 2017). The combination of the two swell regimes results in limited seasonality. This can lead to a rapid decline in observable variability when the survey interval decreases (Almar et al., 2019b), whereas, in the Gulf of Guinea, the Northerly swell does not attain the coast, leaving this part open to Southerly swell with longer fluctuations in wave energy flux (Almar et al., 2015). From the Equator southwards (latitudes 0 to 20S), trade winds play a major role. As a consequence, shorter wave-energy timescales are found.

In addition to temporal variability, waves also have spatial scales (Fig. 4). For example, a storm hitting Western Europe will have an impact at a regional level (i.e. the synoptic scale of the storm and subsequent waves). In the case of morphological change, the impacts can imply varying local morphological changes, but these are regionally linked (Masselink et al., 2016). For instance, there is little added value to survey two closely situated sites if their change is well correlated on a given survey interval scale. Fig. 4 shows the dominant spatial scale, for the dominant temporal scales. The median global dominant spatial scale is 4.8 degrees – representing 540 km at the equator – and shows a great contrast worldwide. The largest values are encountered in the Arabian Sea and the Bay of Bengal around India and the smallest values are found at the transition between the Northern and Southern Atlantic (North

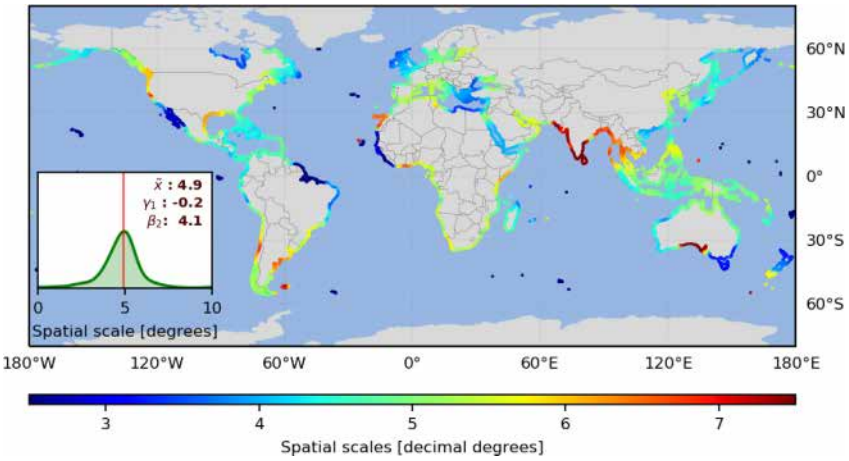

Fig. 4. Global distribution of spatial spheres of influence, the maximum extent of correlated wave time-series (see Methods section). Correlated distance is plotted per location along the world's coastlines including an insert showing the global distribution and median (vertical red line). It is evident from this figure that for the dominant time-scales, correlated wave signals are found within a radius of around 4.9 degrees (550 km at the Equator).

Brazil and part of Western Africa). Small basins and closed seas such as the Mediterranean can be considered as single clusters (with none to limited spatial correlation) as well as islands.

3.2. Uncertainty in monthly coastal monitoring strategies

Long-term ongoing coastal monitoring schemes typically consist of surveys on near-continuous (video camera), monthly, bi-monthly or yearly bases, as, in the case, for instance with hydro-morphological surveys (Splinter et al., 2013; Splinter et al., 2014; Dyer et al., 2016; Abessolo Ondoa et al., 2017; Bergsma et al., 2019b; Biausque and Senechal, 2019; Brodie et al., 2019; Jeanson et al., 2019). The surveying frequency seems to depend on the purpose of the survey: science applications often show a higher surveying frequency than policy-based (district or national) surveys. For beach surveys, for instance, an important question is how much of the wave-induced morphological changes can be captured for each of these surveying frequencies? Fig. 5 shows the global uncertainty (not resolved wave variability) distribution of monthly surveys. (see Fig. 6).

Considering Fig. 5, it is evident that a high uncertainty is linked to a monthly monitoring revisit-interval in a context affected by ocean waves. A vast majority (98.4%) of the globally distributed analysis points have an uncertainty of 50% or higher with a median of 86.9%. Regional patterns in uncertainty can be discerned in Fig. 5 linked to wave-change timescales (Fig. 3). Typically, larger uncertainties are found at regions with shorter – unresolved – wave-change timescales and vice versa. Similar patterns can be found in the cases of weekly and bi-monthly surveying schemes, presented in supplementary Fig. S2. Even weekly surveying schemes, which are inherently likely to be expensive, often exceed the 50% uncertainty threshold.

Monthly observations capture only a fraction of the total wave variability with high uncertainty, and short-timescale coastal changes may be largely missed. Between monthly and bi-monthly surveys, the uncertainty does

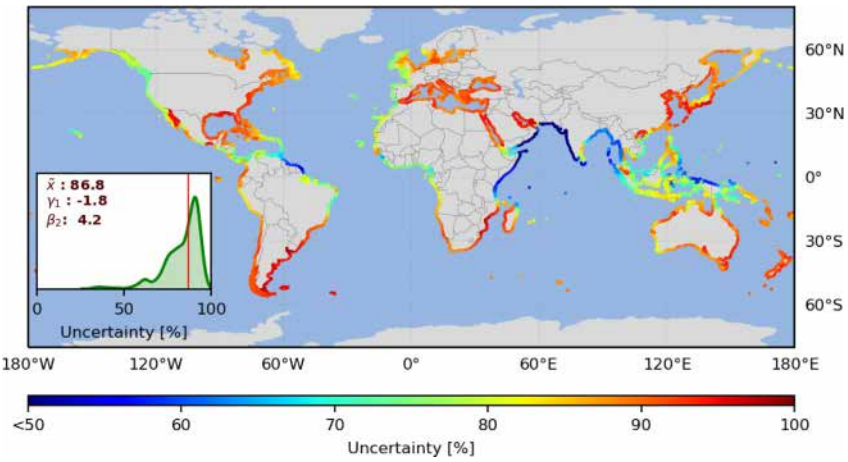

Fig. 5. Global statistical measurement-uncertainty distribution associated with coastal Earth Observation with a monthly interval. It is evident that monthly coastal measurements have high associated uncertainty. The insert highlights this uncertainty: 98.4% of monthly coastal measurements have more than 50% uncertainty. The vertical red line represents the median uncertainty of 86.8%.

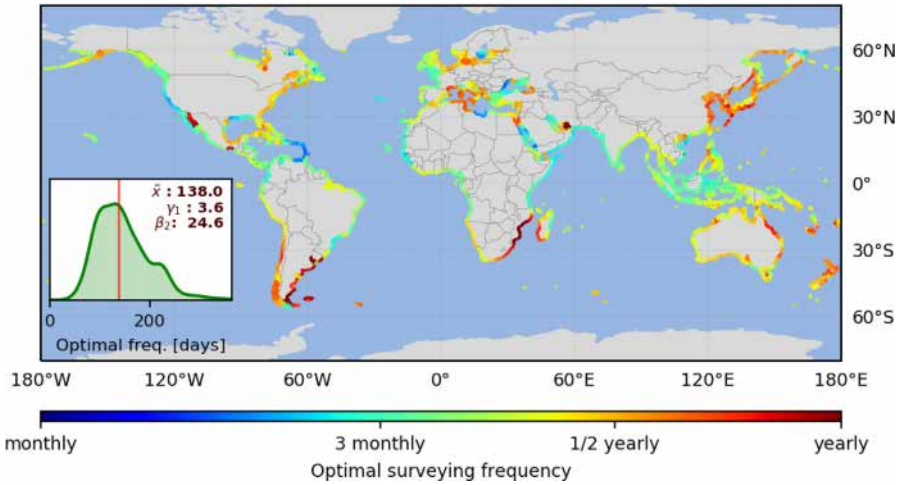

Fig. 6. Global distribution of optimal observational frequency depending on the limited gain/loss of uncertainty. The insert shows the global distribution and the red vertical line represents the median value (138 days).

not further increase at most locations around the world. In other words, it does not matter if a survey is conducted at a bi-monthly or monthly frequency; the observation carries a similar measurement uncertainty. Hence, it is more efficient/optimal to have a lower monitoring frequency while maintaining a similar certainty and conducting surveys on other sites. Following this philosophy, an optimum observational frequency can be found at which we maintain the certainty of the measurement with the lowest observational frequency.

4. Discussion

4.1. Limitations

As a preamble to the discussion, it is important to stress the limitations of our approach. This global analysis gives a first-order vision of coastal wave variability and should be seen as its consequences at wave-exposed open coasts. We have made inevitable simplifications at such a large global scale, using offshore waves and considering regional patterns of coastal wave variability. We have used the global and necessarily coarse publicly available ERAInterim wave hindcast that has been widely used and validated in the literature. We have excluded very high-latitude coasts where wave seasonality is perturbed by sea ice (Ji et al., 2019). We also excluded from our analysis the transformation of wave energy from offshore deep waters to the continental shelves and coastal zones, a process that can be substantial with wide shelves (Passaro et al., 2021b). Here we focus on the regional scales but with a global perspective, under the influence of the same synoptic ocean and atmosphere drivers. Small-scale (spatio-temporal) coastal dynamics can be more complex and out of the reach of the regional scales embodied with this global study. At the regional scale, climate modes such El Nino Southern Oscillation along the Pacific North American coasts (Barnard et al., 2015) drive, for instance, a singular temporal footprint, and energetic winters in the North Atlantic with a succession of storms affect most of the regional West European coasts (Masselink et al., 2016). Other ocean drivers were not accounted for in our study focusing on coastal waves, such as steric and dynamic sea level, including astronomical and atmospheric (surge) tides that can regionally be important drivers of coastal variability (Abessolo Ondoa et al., 2020; Almeida et al., 2020). For example, storm impact depends on when a storm hits the coast, a timing that can be modulated by tidal range (Bertin et al., 2014; Masselink et al., 2016; Bergsma et al., 2019b). Tides also have a more general damping effect in terms of the residence time of wave action. For example, in the microtidal Mediterranean Sea, wave action is concentrated within the restricted tidal excursion range while the large tidal ranges of macrotidal environments generate greater spreading of wave action over the intertidal frame (Karunarathna et al., 2014). In addition, some processes have a delayed response to changes in wave regime, which result in a filter of the highest frequencies. It is in general not the case for hydrodynamical processes such as extreme coastal water levels which respond almost immediately to changes in offshore wave regimes Bertin et al. (2014). Considering morphological wave-induced coastal variability, earlier studies pointed out a certain lag, a response time, between wave conditions and morphological change (Wright and Short, 1984), thus rendering the response less linked to rapid variations of wave energy flux. With observed values around 10-days (Karunarathna et al., 2014), this lag concerns wave fluctuations at higher frequencies corresponding to the ‘event’ scale (days to a week) associated with mid-latitude and tropical storms (Marchesiello et al., 2020), and, thus, non-extant at sub-annual to interannual timescales.

4.2. Way forward for coastal Earth Observation strategies

The lack of spatio-temporal observational data to define global distributions of coastal environment response times

underscores the importance of intensifying observations (Ranasinghe, 2020), through, for instance, space-borne observations (Benveniste et al., 2019; Bergsma et al., 2021), which are particularly feasible for mid- to high latitudes (Bergsma and Almar, 2020). A combined availability of optical satellite data and computational power on cloud platforms (Traganos et al., 2018) enabled a recent global assessment of the erosional state of the world's beaches (Luijendijk et al., 2018). Several possibilities point to a bright future for coastal studies and management (Turner et al., 2021): back-dateable easy access coastal waves, sea-level and current estimations Kudryavtsev et al. (2017), Almar et al. (2021a), Qin and Li (2021) and shoreline detection (Toure et al., 2019; Vos et al., 2019a; Vos et al., 2019b), emerging space-borne topographic restitution (Almeida et al., 2019; Vos et al., 2020; Taveneau et al., 2021; Salameh et al., 2019), increasingly more accurate bathymetry estimation techniques e.g. (Traganos et al., 2018; Caballero and Stumpf, 2019; Almar et al., 2019a; Bergsma et al., 2019a; Almar et al., 2021b), very high-resolution on-demand satellites every day and everywhere on Earth (e.g. Pleiades or Worldview), a Sentinel 2 revisit time at the coast of a maximum 5 days, and often even less, combined with Landsat and data input from dozens of optical cube-satellites. Future radar missions such as SWOT will offer new opportunities to observe the coastal oceanic processes at scales at high frequencies (Morrow et al., 2019). These new advances in satellite technology and the ability to combine Earth observation with numerical and data-based models through assimilation and artificial intelligence will have a major impact on monitoring our coasts on a global basis. At the same time, complementarity with field-based experimental efforts, and empirical knowledge acquired over decades of coastal observation are also important in highlighting some of the inaccuracies inherent in the use of satellite data to characterise aspects of coastal morphology and dynamics, as Cooper et al. (2020) have shown for beaches worldwide, and Castelle et al. (2021) specifically for beaches experiencing large tidal ranges.

5. Conclusion

Coastal waves cover a wide range of coastal environments worldwide. Coastal environments change over a wide range of timescales from storm events, seasonal and inter-annual variability to longer-term adaptation to changing environmental conditions, in particular in response to changing waves. We quantify here global spatio-temporal wave conditions along the world's coasts and assess the need for coastal Earth observation strategies, with the goal, in particular, that derived scales of change can contribute to the optimization of these strategies. A dominant global time scale of 30 days is found in coastal wave variability that is, on average, spatially correlated just above the regional synoptic scale of 5 degrees (about 550 km at the equator). This latter regional-scale dimension suggests that traditional field survey strategies can be supplemented with information obtained from satellite Earth observation. Because Earth observation covers a wide range of space and time scales, it is proving to be an increasingly suitable data source for the coastal environment.

Declaration of Competing Interest

The authors declare that they have no known competing financial interests or personal relationships that could have appeared to influence the work reported in this paper.

Acknowledgement

EB was funded through a CNES-postdoctoral fellowship (CNES - French National Space Agency). All global maps have been created with Metoffice' cartopy package Met Office (2010 - 2019).

Appendix A. Supplementary material

Supplementary data associated with this article can be found, in the online version, at https://doi.org/10.1016/j.asr.2022.02.047.

References

Abessolo Ondoa, G., Almar, R., Jouanno, J., Bonou, F., Castelle, B., Larson, M., 2020. Beach adaptation to intraseasonal sea level changes. Environ. Res. Commun.

Abessolo Ondoa, G., Bonou, F., Tomety, F.S., Du Penhoat, Y., Perret, C., Degbe, C.G.E., Almar, R., 2017. Beach response to wave forcing from event to inter-annual time scales at grand popo, benin (gulf of guinea). Water 9 (6).

Almar, R., Bergsma, E.W.J., Catalan, P.A., Cienfuegos, R., Suarez, L., Lucero, F., Nicolae Lerma, A., Desmazes, F., Perugini, E., Palmsten, M.L., et al., 2021a. Sea state from single optical images: A methodology to derive wind-generated ocean waves from cameras, drones and satellites. Remote Sensing 13 (4), 679.

Almar, R., Bergsma, E.W.J., Maisongrande, P., de Almeida, L.P.M., 2019a. Wave-derived coastal bathymetry from satellite video imagery: A showcase with pleiades persistent mode. Remote Sens. Environ. 231, 111263.

Almar, R., Bergsma, E.W.J., Thoumyre, G., Baba, M.W., Cesbron, G., Daly, C., Garlan, T., Lifermann, A., 2021b. Global satellite-based coastal bathymetry from waves. Remote Sensing 13 (22).

Almar, R., Kestenare, E., Boucharel, J., 2019b. On the key influence of remote climate variability from tropical cyclones, north and south atlantic mid-latitude storms on the senegalese coast (west africa). Environ. Res. Commun. 1 (7), 071001.

Almar, R., Kestenare, E., Reyns, J., Jouanno, J., Anthony, E., Laibi, R., Hemer, M., Du Penhoat, Y., Ranasinghe, R., 2015. Response of the bight of benin (gulf of guinea, west africa) coastline to anthropogenic and natural forcing, part1: Wave climate variability and impacts on the longshore sediment transport. Cont. Shelf Res. 110, 48–59.

Almar, R., Marchesiello, P., Almeida, L.P., Thuan, D.H., Tanaka, H., Viet, N.T., 2017. Shoreline response to a sequence of typhoon and monsoon events. Water 9 (6).

Almar, R., Ranasinghe, R., Bergsma, E.W.J., Diaz, H., Melet, A., Papa, F., Vousdoukas, M., Athanasiou, P., Dada, O., Almeida, L.P., Kestenare, E., 2021c. A global analysis of extreme coastal water levels with implications for potential coastal overtopping. Nature Commun.

Almeida, L.P., Almar, R., Bergsma, E.W.J., Berthier, E., Baptista, P., Garel, E., Dada, O.A., Alves, B., 2019. Deriving high spatial-resolution coastal topography from sub-meter satellite stereo imagery. Remote Sensing 11 (5).

Almeida, L.P., Almar, R., Blenkinsopp, C., Senechal, N., Bergsma, E.W. J., Floch, F., Caulet, C., Biausque, M., Marchesiello, P., Grandjean, P., Ammann, J., Benshila, R., Thuan, D.H., da Silva, P.G., Viet, N.T., 2020. Lidar observations of the swash zone of a low-tide terraced tropical beach under variable wave conditions: the nha trang (vietnam) coastvar experiment. J. Marine Sci. Eng.

Anthony, E., Dussouillez, P., Dolique, F., Besset, M., Brunier, G., Nguyen, V., Goichot, M., 2017. Morphodynamics of an eroding beach and foredune in the mekong river delta: Implications for deltaic shoreline change. Continental Shelf Res. 147, 155–164.

Anthony, E.J., Aagaard, T., 2020. The lower shoreface: Morphodynamics and sediment connectivity with the upper shoreface and beach. Earth Sci. Rev. 210, 103334.

Ardhuin, F., Stopa, J.E., Chapron, B., Collard, F., Husson, R., Jensen, R. E., Johannessen, J., Mouche, A., Passaro, M., Quartly, G.D., Swail, V., Young, I., 2019. Observing sea states. Front. Marine Sci. 6, 124.

Ariffin, E.H., Sedrati, M., Akhir, M.F., Daud, N.R., Yaacob, R., Husain, M.L., 2018. Beach morphodynamics and evolution of monsoon-dominated coasts in kuala terengganu, malaysia: Perspectives for integrated management. Ocean Coastal Manage. 163, 498–514.

Barnard, P.L., Short, A.D., Harley, M.D., Splinter, K.D., Vitousek, S., Turner, I.L., Allan, J., Banno, M., Bryan, K.R., Doria, A., Hansen, J. E., Kato, S., Kuriyama, Y., Randall-Goodwin, E., Ruggiero, P., Walker, I.J., Heathfield, D.K., 2015. Coastal vulnerability across the pacific dominated by el nino/southern oscillation. Nat. Geosci. 8 (10), 801–807.

Benveniste, J., Cazenave, A., Vignudelli, S., Fenoglio-Marc, L., Shah, R., Almar, R., Andersen, O., Birol, F., Bonnefond, P., Bouffard, J., Calafat, F., Cardellach, E., Cipollini, P., Le Cozannet, G., Dufau, C., Fernandes, M.J., Frappart, F., Garrison, J., Gommenginger, C., Han, G., Høyer, J.L., Kourafalou, V., Leuliette, E., Li, Z., Loisel, H., Madsen, K.S., Marcos, M., Melet, A., Meyssignac, B., Pascual, A., Passaro, M., Ribó, S., Scharroo, R., Song, Y.T., Speich, S., Wilkin, J., Woodworth, P., Wöppelmann, G., 2019. Requirements for a coastal hazards observing system. Front. Marine Sci. 6, 348.

Bergsma, E.W., Almar, R., Rolland, A., Binet, R., Brodie, K.L., Bak, A. S., 2021. Coastal morphology from space: A showcase of monitoring the topography-bathymetry continuum. Remote Sens. Environ. 261, 112469.

Bergsma, E.W.J., Almar, R., 2020. Coastal coverage of esa' sentinel 2 mission. Adv. Space Res.

Bergsma, E.W.J., Almar, R., Maisongrande, P., 2019a. Radon-augmented sentinel-2 satellite imagery to derive wave-patterns and regional bathymetry. Remote Sensing 11 (16).

Bergsma, E.W.J., Conley, D.C., Davidson, M.A., OHare, T.J., Almar, R., 2019b. Storm event to seasonal evolution of nearshore bathymetry derived from shore-based video imagery. Remote Sensing 11 (5).

Bertin, X., Li, K., Roland, A., Zhang, Y.J., Breilh, J.F., Chaumillon, E., 2014. A modeling-based analysis of the flooding associated with xynthia, central bay of biscay. Coast. Eng. 94, 80–89.

Biausque, M., Senechal, N., 2019. Seasonal morphological response of an open sandy beach to winter wave conditions: The example of biscarrosse beach, sw france. Geomorphology 332, 157–169.

Boucharel, J., Santiago, L., Almar, R., Kestenare, E., 2021. Coastal wave extremes around the pacific and their remote seasonal connection to climate modes. Climate 9 (12).

Brodie, K., Conery, I., Cohn, N., Spore, N., Palmsten, M., 2019. Spatial variability of coastal foredune evolution, part a: Timescales of months to years. J. Marine Sci. Eng. 7 (5).

Caballero, I., Stumpf, R.P., 2019. Retrieval of nearshore bathymetry from sentinel-2a and 2b satellites in south florida coastal waters. Estuar. Coast. Shelf Sci. 226, 106277.

Castelle, B., Masselink, G., Scott, T., Stokes, C., Konstantinou, A., Marieu, V., Bujan, S., 2021. Satellite-derived shoreline detection at a high-energy meso-macrotidal beach. Geomorphology 383, 107707.

Cooper, J.A.G., Masselink, G., Coco, G., Short, A.D., Castelle, B., Rogers, K., Anthony, E., Green, A.N., Kelley, J.T., Pilkey, O.H., Jackson, D.W.T., 2020. Sandy beaches can survive sea-level rise. Nature Climate Change 10 (11), 993–995.

Davidson, M., Splinter, K., Turner, I., 2013. A simple equilibrium model for predicting shoreline change. Coast. Eng. 73, 191–202.

Davies, J., 1980. Geographical Variation to Coastal Development, 2nd Edition. Longman (Pearson Education Limited).

Dee, D.P., Uppala, S.M., Simmons, A.J., Berrisford, P., Poli, P., Kobayashi, S., Andrae, U., Balmaseda, M.A., Balsamo, G., Bauer, P., Bechtold, P., Beljaars, A.C.M., van de Berg, L., Bidlot, J., Bormann, N., Delsol, C., Dragani, R., Fuentes, M., Geer, A.J., Haimberger, L., Healy, S.B., Hersbach, H., Hólm, E.V., Isaksen, L., Kållberg, P., Köhler, M., Matricardi, M., McNally, A.P., Monge-Sanz, B.M., Morcrette, J.-J., Park, B.-K., Peubey, C., de Rosnay, P., Tavolato, C., Thépaut, J.-N., Vitart, F., 2011. The era-interim reanalysis: configuration and performance of the data assimilation system. Quarterly J. Roy. Meteorol. Soc. 137 (656), 553–597.

Dyer, T., Brodie, K.L., Spore, N., Feb. 2016. Near Real-Time Collection, Processing, and Publication of Beach Morphology and Oceanographic LIDAR Data. In: American Geophysical Union, Ocean Sciences Meeting 2016, abstract #OD24C-2476.

Hoskins, B.J., Hodges, K.I., 2005. A new perspective on southern hemisphere storm tracks. J. Clim. 18 (20), 4108–4129.

Hoskins, B.J., Hodges, K.I., 2019a. The annual cycle of northern hemisphere storm tracks. part i: Seasons. J. Clim. 32 (6), 1743–1760.

Hoskins, B.J., Hodges, K.I., 2019b. The annual cycle of northern hemisphere storm tracks. part ii: Regional detail. J. Clim. 32 (6), 1761–1775.

Jeanson, M., Anthony, E.J., Dolique, F., Aubry, A., 2013. Wave characteristics and morphological variations of pocket beaches in a coral reef-lagoon setting, mayotte island, indian ocean. Geomorphology 182, 190–209.

Jeanson, M., Dolique, F., Anthony, E.J., Aubry, A., 2019. Decadal-scale Dynamics and Morphological Evolution of Mangroves and Beaches in a Reef-lagoon Complex, Mayotte Island. J. Coastal Res. 88 (sp1), 195–208.

Ji, X., Gronewold, A.D., Daher, H., Rood, R.B., 2019. Modeling seasonal onset of coastal ice. Climatic Change 154 (1), 125–141.

Karunarathna, H., Pender, D., Ranasinghe, R., Short, A.D., Reeve, D.E., 2014. The effects of storm clustering on beach profile variability. Mar. Geol. 348, 103–112.

Kudryavtsev, V., Yurovskaya, M., Chapron, B.F.C., Donlon, C., 2017. Sun glitter imagery of ocean surface waves. part 1: Directional spectrum retrieval and validation. J. Geophys. Res.-Oceans 122 (2), 1369–1383.

Luijendijk, A., Hagenaars, G., Ranasinghe, R., Baart, F., Donchyts, G., Aarninkhof, S., 2018. The state of the world's beaches. Nature, Sci. Rep., 8 article 6641

Marchesiello, P., Kestenare, E., Almar, R., Boucharel, J., Nguyen, N.M., 2020. Longshore drift produced by climate-modulated monsoons and typhoons in the south china sea. J. Mar. Syst. 211, 103399.

Masselink, G., Scott, T., Poate, T., Russell, P., Davidson, M., Conley, D., 2016. The extreme 2013/2014 winter storms: hydrodynamic forcing and coastal response along the southwest coast of england. Earth Surf. Proc. Land. 41 (3), 378–391.

Melet, A., Teatini, P., Le Cozannet, G., Jamet, C., Conversi, A., Benveniste, J., Almar, R., 2020. Earth observations for monitoring marine coastal hazards and their drivers. Surv. Geophys. 41 (6), 1489–1534.

Met Office, 2010 - 2019. Cartopy: a cartographic python library with a matplotlib interface. Exeter, Devon. URL http://scitools.org.uk/cartopy.

Morrow, R., Fu, L.-L., Ardhuin, F., Benkiran, M., Chapron, B., Cosme, E., d'Ovidio, F., Farrar, J.T., Gille, S.T., Lapeyre, G., et al., 2019.

Global observations of fine-scale ocean surface topography with the surface water and ocean topography (swot) mission. Front. Marine Sci. 6, 232.
O'Kane, T.J., Matear, R.J., Chamberlain, M.A., Oliver, E.C.J., Holbrook, N.J., 2014. Storm tracks in the southern hemisphere subtropical oceans. J. Geophys. Res.: Oceans 119 (9), 6078–6100.
Passaro, M., Hemer, M.A., Quartly, G.D., Schwatke, C., Dettmering, D., Seitz, F., 2021a. Global coastal attenuation of wind-waves observed with radar altimetry. Nature Commun. 12 (1), 3812.
Passaro, M., Hemer, M.A., Quartly, G.D., Schwatke, C., Dettmering, D., Seitz, F., 2021b. Global coastal attenuation of wind-waves observed with radar altimetry. Nature Commun. 12 (1), 3812.
Qin, L., Li, Y., 2021. Significant wave height estimation using multi-satellite observations from gnss-r. Remote Sensing 13 (23).
Ranasinghe, R., 2020. On the need for a new generation of coastal change models for the 21st century. Sci. Rep. 10 (1), 2010.
Reguero, B., Losada, I., Méndez, F., 2015. A global wave power resource and its seasonal, interannual and long-term variability. Appl. Energy 148, 366–380.
Sadio, M., Anthony, E.J., Diaw, A.T., Dussouillez, P., Fleury, J.T., Kane, A., Almar, R., Kestenare, E., 2017. Shoreline changes on the wave-influenced senegal river delta, west africa: The roles of natural processes and human interventions. Water 9 (5).
Salameh, E., Frappart, F., Almar, R., Baptista, P., Heygster, G., Lubac, B., Raucoules, D., Almeida, L.P., Bergsma, E.W.J., Capo, S., De Michele, M., Idier, D., Li, Z., Marieu, V., Poupardin, A., Silva, P.A., Turki, I., Laignel, B., 2019. Monitoring beach topography and nearshore bathymetry using spaceborne remote sensing: A review. Remote Sens. 11 (19).
Splinter, K.D., Turner, I.L., Davidson, M.A., 2013. How much data is enough? the importance of morphological sampling interval and duration for calibration of empirical shoreline models. Coast. Eng. 77, 14–27.
Splinter, K.D., Turner, I.L., Davidson, M.A., Barnard, P., Castelle, B., Oltman-Shay, J., 2014. A generalized equilibrium model for predicting daily to interannual shoreline response. J. Geophys. Res.: Earth Surface 119 (9), 1936–1958.
Stopa, J.E., Cheung, K.F., 2014. Periodicity and patterns of ocean wind and wave climate. J. Geophys. Res.: Oceans 119 (8), 5563–5584.
Taveneau, A., Almar, R., Bergsma, E.W.J., Sy, B.A., Ndour, A., Sadio, M., Garlan, T., 2021. Observing and predicting coastal erosion at the langue de barbarie sand spit around saint louis (senegal, west africa) through satellite-derived digital elevation model and shoreline. Remote Sensing 13 (13).
Toure, S., Diop, O., Kpalma, K., Maiga, A.S., 2019. Shoreline detection using optical remote sensing: A review. ISPRS Int. J. Geo-Informat. 8 (2).
Traganos, D., Poursanidis, D., Aggarwal, B., Chrysoulakis, N., Reinartz, P., 2018. Estimating satellite-derived bathymetry (sdb) with the google earth engine and sentinel-2. Remote Sensing 10 (6).
Turner, I.L., Harley, M.D., Almar, R., Bergsma, E.W., 2021. Satellite optical imagery in coastal engineering. Coast. Eng. 167, 103919.
Vos, K., Harley, M.D., Splinter, K.D., Simmons, J.A., Turner, I.L., 2019a. Sub-annual to multi-decadal shoreline variability from publicly available satellite imagery. Coast. Eng. 150, 160–174.
Vos, K., Harley, M.D., Splinter, K.D., Walker, A., Turner, I.L., 2020. Beach slopes from satellite-derived shorelines. Geophys. Res. Lett. 47 (14), e2020GL088365, e2020GL088365 2020GL088365.
Vos, K., Splinter, K.D., Harley, M.D., Simmons, J.A., Turner, I.L., 2019b. Coastsat: A google earth engine-enabled python toolkit to extract shorelines from publicly available satellite imagery. Environ. Modell. Softw. 122, 104528.
Wright, L., Short, A.D., 1984. Morphodynamic variability of surf zones and beaches; a synthesis. Mar. Geol. 56, 93–118.
Young, I.R., Zieger, S., Babanin, A.V., 2011. Global trends in wind speed and wave height. Science 332 (6028), 451–455.